EUROPEAN ORGANIZATION FOR NUCLEAR RESEARCH
CERN – ACCELERATORS AND TECHNOLOGY SECTOR

CERN-ATS-2012-075

Local chromatic correction scheme and crab-waist collisions for an ultra-low beta* at the LHC

J.L. Abelleira, EPFL & CERN;
S. Russenschuck, R. Tomas, F. Zimmermann, CERN, Switzerland;
K. Ohmi, KEK, Japan; C. Milardi, M. Zobov, INFN-LNF, Italy;
D. Shatilov, BINP, Russia

Abstract

We discuss potential merits and the parameter range of interest for a possible crab-waist collision scheme at the LHC, and report preliminary optics studies of a local chromatic correction scheme with flat beams ($\beta^*_x \gg \beta^*_y$), which could boost the LHC luminosity by about an order of magnitude and would also allow for crab-waist collisions.

Presented at the International Particle Accelerator Conference (IPAC'12) –

May 20-25, 2012, N. Orleans, USA

Geneva, Switzerland, May 2012

LOCAL CHROMATIC CORRECTION SCHEME AND CRAB-WAIST COLLISIONS FOR AN ULTRA-LOW BETA* AT THE LHC*

J.L. Abelleira, EPFL & CERN; S. Russenschuck, R. Tomas, F. Zimmermann, CERN, Switzerland; K. Ohmi, KEK, Japan; C. Milardi, M. Zobov, INFN-LNF, Italy; D. Shatilov, BINP, Russia

Abstract

We discuss potential merits and the parameter range of interest for a possible crab-waist collision scheme at the LHC, and report preliminary optics studies of a local chromatic correction scheme with flat beams ($\beta_x^* \gg \beta_y^*$), which could boost the LHC luminosity by about an order of magnitude and would also allow for crab-waist collisions.

INTRODUCTION

A novel direction to increase the LHC luminosity through a change of the insertion regions (IRs) 1 and 5 combines several components.

The first component is a large Piwinski angle (LPA), which decreases the overlapping area of the bunches at collision point. The second component, an extremely low β_y^* fitting the overlapping area, will lead to flat-beam optics in collision, and is the main source of the luminosity increase. The low β_y^* can be realized with a local correction scheme in the vertical plane – the third component. Finally, the fourth component is a crab-waist (C-W) collision scheme, which suppresses beam-beam driven betatron resonances and potentially allows for higher values of the beam-beam tune shift to be reached with an associated additional luminosity increase. Crab-waist collisions require a large Piwinski angle and extremely flat collisions, which are provided by the first three components.

The big challenge is moving from a round-beam to a flat beam optics in proton-proton collisions.

PARAMETERS

Tentative interaction-point (IP) parameters were constructed starting from the requirement $\sigma_x^*/\sigma_y^* \geq 10$ [1] and $\beta_x^*\beta_y^* \leq (0.15\ \mathrm{m})^2$, also taking into account a preliminary design of the final quadrupole (see below).

These strawman parameters are listed in Table 1, where θ_c represents the full crossing angle and $\phi \equiv \theta\sigma_z/(2\sigma_x^*)$ the Piwinski angle.

Table 1: IP parameters for novel LHC optics.

$\beta_{x,y}^*$	1.5, 0.015 m
θ_c	4 mrad
$\epsilon_{N;x,y}$	2.2–3.75 μm
$\sigma_{x,y}^*$	15.2–26.0, 2.0-3.5 μm
σ_z	7.55 cm
ϕ	5.8–9.9

* Work supported by the European Commission under the FP7 Research Infrastructures project EuCARD, grant agreement no. 227579.

CRAB-WAIST OPTICS

Figure 1 shows the beta functions and dispersion on the right side of the IP, matched to the right part of the arc. The optics on the left side and the one for the other beam have to be matched separately. This symmetric optics is quite different from the antisymmetric LHC design optics. Details of the new optics development are given in [2].

In particular some bending dipoles are added to the straight section in order to make the design trajectories of the two beams intersect at the desired large crossing angle, in contrast to the actual LHC where, without IR bumps, the two closed orbits are identical between the first (separation) dipole D1 and the IP. The strengths of these bending magnets have also been adjusted so as to match the value of the dispersion and its angle at the entrance of the arc.

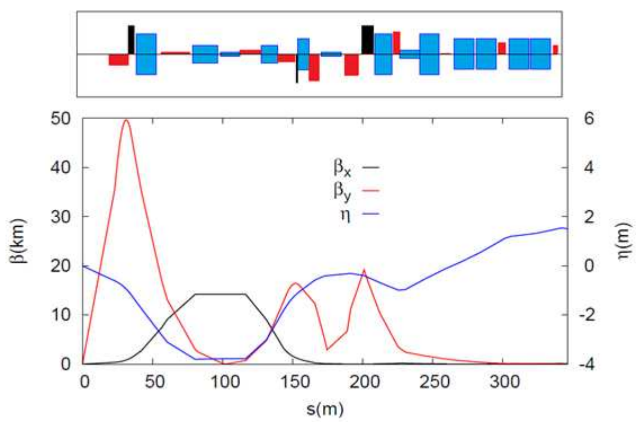

Figure 1: LHC flat-beam IR optics (right side of the IP). Bending magnets are shown in blue, quadrupoles in red and sextupoles in black.

The three peaks in the β-functions roughly correspond to the locations of three sextupoles. The betatron phase advances between these sextupoles (denoted sext1, sext2, and sex3 in Table 2) are important and were used as a design constraint. The first two sextupoles are used for a local chromatic correction in the vertical plane, by matching their strengths and the value of the dispersion at the sextupole locations. The phase advance between sext2 and sext1 is such that the geometric aberrations can be cancelled. The additional third sextupole has the proper phase advance from the IP to realize a crab waist collision.

The equivalent third sextupole (sext3) on the other side of the IP is excited with the opposite polarity so that the crab-waist aberration is compensated and the perturbation remains local. When this sextupole is excited, the chromatic correction and the other geometric aberrations, e.g. y^3 terms in the Hamiltonian, need to be re-optimized by re-adjusting the strengths of the first two sextupoles. Specifically, the three sextupole strengths (plus those on the other side of the IP) can be combined into a "multiknob," which only varies the crab-waist shift at the IP and leaves all other relevant aberrations unchanged.

The geometry of the new IR is shown in Fig. 2.

Table 2: Betatron phase advances from the IP to the three sextupoles

	sext1	sext2	sext3
$\Delta\mu_x$	$\pi/2$	$\pi/2$	π
$\Delta\mu_y$	$\pi/2$	$3\pi/2$	$5\pi/2$

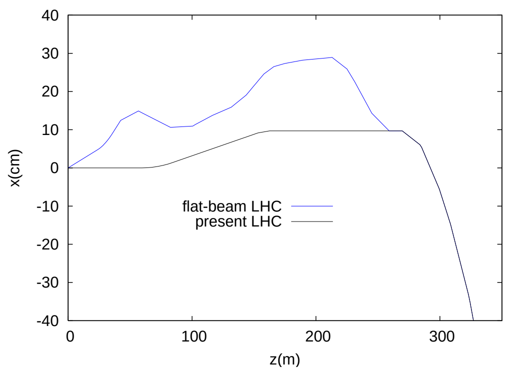

Figure 2: Reference orbit comparison with actual LHC

FINAL QUADRUPOLE

In the present LHC IRs, the two beams travel through the same aperture and experience the same field in the final-triplet quadrupoles. The horizontal optics for beam 1 is the same as the vertical for beam 2 on the same side of the IP, and the same as the beam-2 horizontal optics on the other side.

In contrast to the present LHC configuration, a flat-beam optics requires a symmetric optics for the two beams, e.g. the same optical functions for both beams and on both sides of the IP. Keeping the free length from the IP to the entrance face of the first quadrupole, l^{P*}, equal to its present value of about 23 m, the beam separation at this location is $l^*\theta_c = 90$ mm, which is not sufficient for installing two regular SC quadrupoles of opposite polarity. Inspired by the LHeC "half-quadrupole" design [3], a "double half quadrupole" is considered. Choosing a rectangular aperture (which would not be possible with a pure sextupole geometry), allows accommodating two side-by-side beam pipes of elliptic dimensions.

For small gradients and apertures half-quadrupoles can be constructed with a mirror-plate from soft-magnetic steel. This type of magnet was installed in the IRs of the HERA ep collider [4] and of the KEK B-factory [5]. However, the required gradient makes it necessary to apply superconductor technology for the coils, and would also result in a complete saturation of the mirror-plate. Therefore, we have developed a combined function magnet consisting of eight racetrack coils that produce a combined dipole and sextupole field in the common aperture; see Fig. 3.

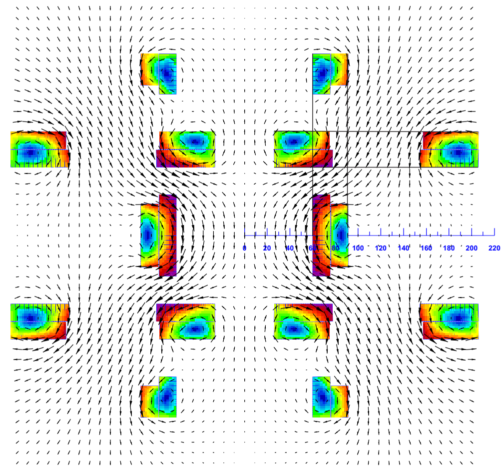

Figure 3: Cross-section of a double half-quadrupole. The coils are wound from simple racetracks in order to facility the production in case Nb_3Sn superconductor technology would be required.

We assume LHC innner and outer layer Nb-Ti cable, operated at 80% on the load-line. The peak field in the coil is 8.14 T for an aperture square of 160 mm, and the gradient at the center of the beam (45 mm from the origin) is 116 T/m, with an additional dipole field component of 5.5 T.

Analytical solutions are available for producing field configurations with two beams of minimum separation by the optimized placement of individual SC wires [6]. The simple (non-optimum) racetrack shape chosen for the SC coils of Fig. 3 will facilitate the use of Nb_3Sn technology if required. The field distribution of the double half-qadrupole is shown in Fig. 4 [7]. Since the design orbits of the two beams are separated by 90 mm, the feed-down from the strong sextupole produces the desired strong quadrupole component. The inherent sextupole field must be added to the field of the first sextupole, "sext1."

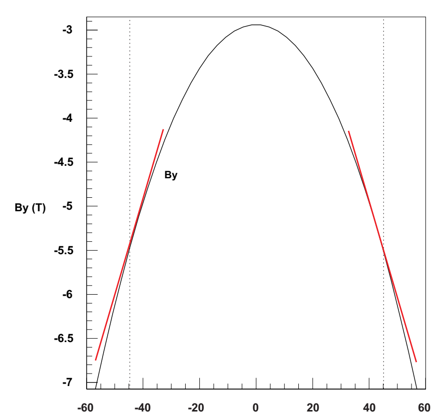

Figure 4: Magnetic field distribution for the double half-quadrupole, computed by ROXIE.

LPA AND C-W COLLISIONS

The large Piwinski angle not only reduces the geometric luminosity, but also the beam-beam tune shift. Therefore, a higher brightness can be accepted, with the net effect of increasing the luminosity [8]. Most importantly the overlap area of the colliding bunches is reduced, to become roughly equal to σ_x^*/θ_c. Then β_y^* can be made comparable to the overlap area size (i.e. much smaller than the bunch length), or $\beta_y^* \approx 2\sigma_x^*/\theta \ll \sigma_z$ [9].

However, the large Piwinski angle itself introduces new beam-beam resonances, arising (in collisions without C-W) through the vertical motion modulation by the horizontal oscillations which are suppressed by the C-W transformation [10]. Crab-waist collisions were successfully implemented at the DAϕNE e^+e^- collider [11].

BEAM-BEAM SIMULATIONS

We used the Frequency Map Analysis (FMA) [12] to explore beam dynamics in the LHC. Beam-beam simulations with a crab waist showed [1] that for the equal-emittance beams of the LHC, a β^* ratio of at least 100 is needed for the crab-waist sextupole to be effective in suppressing beam-beam resonances. Figures 5 and 6 show an example for θ_c = 1.5 mrad. Here tune-diffusion values are plotted in two different planes: in the plane of the betatron tunes, i.e. the so-called tune foot prints (left pictures) and the plane of normalized betatron amplitudes (right pictures). Figure 5 refers to a situation without crab-waist sextupoles, while Fig. 6 shows a case in which the sextupoles are switched on at 50% of their nominal strength. The blue color indicates stable motion and the red color signifies stochasticity.

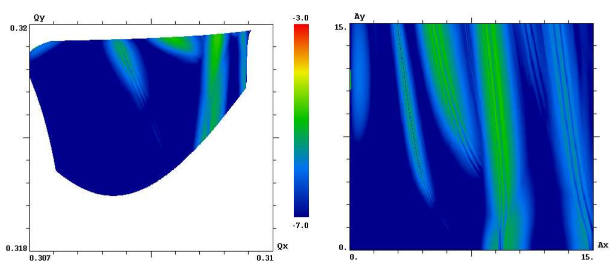

Figure 5: Resonance plot without crab waist.

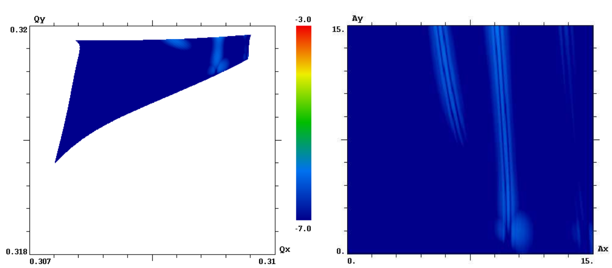

Figure 6: Resonance plot with crab waist.

As we can see switching on the crab-waist sextupoles has two beneficial consequences: a smaller footprint area and a considerable reduction of the beam-beam resonance strength. By exploiting the crab sextupoles one can expect a better beam-beam performance in terms of luminosity and beam lifetime, as well as the potential of higher beam-beam tune shifts.

LUMINOSITY GAIN

Table 3 shows the peak luminosity for a full crossing angle of θ_c equal to 4 mrad. The luminosity is lower than what it would be at the same bunch intensity N_b and normalized emittance ϵ_N with the nominal LHC optics ($\beta^*_{x,y}$ = 0.55 m,θ_c = 285μrad). The primary limitation is the half quadrupole aperture. If further magnet designs reduce the necessary crosing angle, for example by using Nb_3Sn instead of Nb-Ti in the double half quadrupole, a significant luminosity increase can be obtained. The gain for θ_c = 2 mrad is also indicated.

Table 3: Luminosity [10^{34} cm^{-2}s^{-1}] for θ_c = 4 (2) mrad.

$N_b[10^{11}] \setminus \epsilon_N[\mu\mathrm{m}]$	3.75	3.00	2.20
1.15	0.6 (1.1)	0.8 (1.5)	1.1 (2.1)
2.0	1.9 (3.5)	2.4 (4.5)	3.2 (6.3)
3.0	4.2 (7.8)	5.3 (10)	7.3 (14)

CONCLUSIONS

We have presented a first strawman design for a new LHC IR optics with three novel features: (1) extremely flat beams, (2) local chromatic correction in one plane, and (3) a crab-waist sextupole. This optics is compatible with the preliminary design of a double half quadrupole to be placed closest to the IP. It also complies with the constraints from LHC beam-beam simulations. The new IR scheme could increase the LHC peak luminosity by up to a factor of 10. It also is an interesting and attractive options for a future High-Energy LHC (HE-LHC) [13], where the beams are naturally flat ($\epsilon_y \ll \epsilon_x$) due to synchrotron radiation.

REFERENCES

[1] D. Shatilov, et al, PRST-AB 14:014001 (2011)

[2] J.L. Abelleira, EuCARD 2012 Annual Meeting

[3] LHeC Study Group, C. Adolphsen et al, LHeC-Note-2011-003 GEN, CERN, 2011, to be published.

[4] E. Bondarchuk et al, Proc. EPAC'98 Stockholm, p. 1972

[5] K. Kanazawa et al, NIMA 499 (2003) 75–99

[6] S. Fartoukh, LHC Project Report 1012 (2007)

[7] S. Russenschuck, Field Computation for Accelerator Magnets, Wiley-VCH 2010

[8] F. Ruggiero, F. Zimmermann, PRST-AB 5:061001 (2002)

[9] P. Raimondi, Proc. EPAC08, Genoa, p. 1898

[10] P. Raimondi et al, LNF-07-003-IR, physics/0702033 (2007)

[11] M. Zobov et al, Phys.Rev.Lett. 104:174801 (2010)

[12] J. Laskar, Icarus 88, 266 (1990).

[13] R. Assmann et al, "First Thoughts on a Higher-Energy LHC," CERN-ATS-2010-177 (2010)